

Nrf2 deficiency causes tooth decolorization due to iron transport disorder in enamel organ

Toru Yanagawa¹, Ken Itoh^{2, 3}, Junya Uwayama¹, Yasuaki Shibata⁴, Akira Yamaguchi⁴, Tsuneyoshi Sano⁵, Tetsuro Ishii⁶, Hiroshi Yoshida¹ and Masayuki Yamamoto^{2, 3, *}

¹Institute of Clinical Medicine, ²JST-ERATO Environmental Response Project, ³Institute of Basic Medical Sciences and Center for Tsukuba Advanced Research Alliance, University of Tsukuba, 1-1-1 Tennoudai, Tsukuba 305-8575, ⁴Division of Oral Pathology and Bone Metabolism, Department of Developmental and Reconstructive Medicine, Nagasaki University Graduate School of Biomedical Sciences, 1-7-1 Sakamoto, Nagasaki, 852-8588, ⁵Department of Oral Anatomy, Showa University School of Dentistry, 1-5-8 Hatanodai, Shinagawa-ku, Tokyo 142-8585, and ⁶Institute of Community Medicine, University of Tsukuba, 1-1-1 Tennoudai, Tsukuba 305-8577, Japan

Running head: Nrf2 regulation of iron transport

Key words: ameloblast, iron transport, Nrf2

*Corresponding author

Please send proofs to:

Masayuki Yamamoto, M.D., Ph.D.,
Center for TARA and Institute of Basic Medical Sciences,
University of Tsukuba, 1-1-1 Tennoudai, Tsukuba 305-8577, Japan
Phone 81-298-53-6158; FAX 81-298-53-7318
E-mail: masi@tara.tsukuba.ac.jp

Abstract

Rodents have brownish-yellow incisors whose color represents their iron content. Iron is deposited into the mature enamel by ameloblasts that outline enamel surface of the teeth. Nrf2 is a basic region-leucine zipper type transcription factor that regulates expression of a range of cytoprotective genes in response to oxidative and xenobiotic stresses. We found that genetically engineered Nrf2-deficient mice show decolorization of the incisors. While incisors of wild type mice were brownish yellow, incisors of Nrf2-deficient mice were grayish white in color. Micro X-ray imaging analysis revealed that the iron content in Nrf2-deficient mouse incisors were significantly decreased compared to that of wild type mice. We found that iron was aberrantly deposited in the papillary layer cells of enamel organ in Nrf2-deficient mouse, suggesting that the iron transport from blood vessels to ameloblasts was disturbed. We also found that ameloblasts of Nrf2-null mouse show degenerative atrophy at the late maturation stage, which gives rise to the loss of iron deposition to the surface of mature enamel. Our results thus demonstrate that the enamel organ of Nrf2-deficient mouse has a reduced iron transport capacity, which results in both the enamel cell degeneration and disturbance of iron deposition onto the enamel surface.

Introduction

The brownish yellow color of the rodent incisors is owing to iron deposition in the enamel surface layer (Halse, 1973; Halse, 1974; Halse & Selvig, K. A. 1974; Kallenbach, 1970). In the enamel organ of rodents, where the tooth develops, a layer of cells that outline the enamel surface called ameloblasts contain the entire sequence of cell development stages. From the apical end toward the incisal end these stages are classified regionally into presecretory, secretory, transition, and maturation stages. Secretory ameloblasts produce enamel matrix proteins, whereas ameloblasts at the maturation stage act to incorporate iron and deposit it into the surface of the mature enamel, in addition to their fundamental roles in enamel formation. In this unique iron transport system, ferritin functions as a transient iron reservoir in the cell, sequestering iron into the cytoplasmic granules (Karim & Warshawsky, 1984). This particle first appears free in the cytoplasm, and then gradually becomes confined to the membrane bound ferritin-containing vesicles with the progression of cell developmental stages. Finally, the iron is secreted from ameloblasts into the enamel surface at the end of maturation, presumably through the process of lysosomal digestion of ferritin (Takano & Ozawa, 1981).

Iron is critically involved in a wide variety of cellular events ranging from DNA synthesis to cellular respiration (Cammack *et al.* 1990). However, at the same time, free iron generates highly reactive oxygen species via Fenton chemistry and causes an oxidative stress to cells (Linn *et al.* 1998). Thus, the cellular iron metabolism should be strictly regulated in the presence of various transport and

storage proteins (McCord, 1998).

Nrf2 belongs to the CNC transcription factor family which share a characteristic basic domain first identified in the *Drosophila* cap'n'collar (CNC) protein (Itoh *et al.* 1995, Mohler *et al.* 1991). Nrf2 is essential for the coordinate transcriptional induction of phase II enzymes and antioxidant genes via antioxidant responsive element (ARE) (Itoh *et al.* 1997, Ishii *et al.* 2000). Furthermore, Nrf2 constitutes a crucial cellular sensor for oxidative stress together with its cytoplasmic repressor Keap1, and mediates a key step in the signaling pathway by a novel Nrf2 nuclear shuttling mechanism (Itoh *et al.* 1999b). Activation of Nrf2 leads to the induction of phase II enzyme and antioxidant stress genes in response to various stresses (Ishii *et al.* 2000; Itoh *et al.* 1999a).

Whereas Nrf2-deficient mice (*Nrf2*^{-/-}) grow normally and are fertile (Itoh *et al.* 1997), the mice are susceptible to various oxidative stresses including acetaminophen intoxication (Enomoto *et al.* 2001; Chan *et al.* 2001), BHT intoxication (Chan *et al.* 1998), chemical carcinogenesis (Ramos-Gomez *et al.* 2001), hyperoxia (Cho *et al.* 2002), and diesel exhaust inhalation (Aoki *et al.* 2001). The *Nrf2*^{-/-} mice are also susceptible to lupus-like autoimmune nephritis (Yoh *et al.* 2001). However, no apparent phenotype has yet been described (Itoh *et al.* 1997; Kuroha *et al.* 1998). In this study, we found that incisors of the *Nrf2*^{-/-} mice are decolorized and become grayish white. The examination of the mechanisms leading to the decolorization in the *Nrf2*^{-/-} mouse revealed that the iron transport is defective in the developing enamel organ of *Nrf2*^{-/-} mice.

Results

Decolorization of the maxillary incisors of *Nrf2*^{-/-} mice

In an attempt to find subtle anatomical changes in the germ line *Nrf2*^{-/-} mice (Itoh *et al.* 1997), we noticed that the incisors of *Nrf2*^{-/-} mice are always grayish white (Fig. 1B), while in contrast, incisors of wild-type and heterozygous mutant (*Nrf2*^{+/-}) mice are always brownish yellow (Fig. 1A). In order to examine the decolorization phenotype in more detail, we mated *Nrf2*^{+/-} male with *Nrf2*^{+/-} female mice and examined 50 mice for the relationship between *Nrf2* genotype and the incidence of decolorization by macroscopic examination. Fourteen mice had grayish-white incisors and all of them were homozygous for the *Nrf2* germ line mutation. On the contrary, of the 36 mice with brownish yellow incisors, 26 were *Nrf2* heterozygous and 10 were wild type. Thus, the penetration of decolorization phenotype in *Nrf2*^{-/-} mice was 100% (P<0.001).

Iron content in enamel surface was specifically decreased in *Nrf2*^{-/-} mice

Scanning electron microscopic analysis detected no significant structural differences in the tooth surface between wild-type (Fig. 2A) and *Nrf2*^{-/-} mice (Fig. 2D). However, X-ray microanalysis revealed an apparent difference in the iron content on the enamel surfaces between the *Nrf2*^{-/-} and wild-type mice (Table 1). A dot-map image analysis revealed the remarkable decrease of iron content in the enamel surface of *Nrf2*^{-/-} mouse incisors (Fig. 2F) compared to those of wild-type mice (Fig. 2C). Calcium content was within comparable range between wild-type (Fig. 2B) and *Nrf2*^{-/-} mice (Fig. 2E).

Table 1 summarizes the calcium, phosphorus and iron contents of the incisors that were quantified by X-ray microanalysis. Importantly, we found that the mean iron content (weight %) of the *Nrf2*^{-/-} mouse enamel was less than one-tenth of that of the wild-type mouse. The decrease shows gene copy number dependence such that in the *Nrf2*^{+/-} mouse incisors the mean iron content was about one half of that of the wild-type mice. In contrast, no significant difference was observed in the content of calcium and phosphorus amongst *Nrf2*^{-/-}, *Nrf2*^{+/-} and wild-type mice. Similarly, the molar ratio (MR) as well as weight % ratio (WR) of calcium to potassium was unaffected. These results indicate that the iron metabolism is specifically affected in the *Nrf2*^{-/-} mouse teeth.

General iron status in *Nrf2*^{-/-} mice

To examine the reason why the iron metabolism of enamel organ was impaired in *Nrf2*^{-/-} mice, we measured the general iron status in *Nrf2*^{-/-} mice. We did not find any significant differences in hematocrit, serum iron concentration, total iron binding capacity (TIBC) and transferrin saturation (Table 2), indicating that the general iron status of *Nrf2*^{-/-} mice is not affected. In contrast, non-heme iron content of liver was found to be significantly higher in *Nrf2*^{-/-} mice than that in wild-type liver. The precise reason of this iron increase in the liver remains to be clarified.

Ameloblasts of *Nrf2*^{-/-} mice show premature degenerative atrophy

We next examined development of ameloblasts in *Nrf2*^{-/-} mouse, since it is ameloblasts that deposit iron into the enamel surface. A histological examination with lower magnification of wild-type mouse tissues with hematoxylin and eosin staining showed slight signs of degenerative atrophy in the late maturation stage of the ameloblast development (**Im**, Fig. **3A**). Compared to the wild-type mice, however, these changes in the *Nrf2*^{-/-} mouse ameloblasts were abrupt and premature (below). We found that, while ameloblasts of *Nrf2*^{-/-} mice showed very similar morphological appearance to that of the wild-type mice during the transition (**t**) stage and the early maturation (**em**) stage, ameloblasts of *Nrf2*^{-/-} mice suffered severely from premature degenerative atrophy at the late maturation stage (Fig. **3B**; green arrow). The late maturation stage is the time when iron is excreted from ameloblasts to the enamel surface. At higher magnification, cell heights of ameloblasts gradually reduced from the early maturation stage to the late maturation stage in wild type ameloblasts. At the stages of reduced ameloblasts, they were changed to atrophic flat squamous cells on the most incisal side. In agreement with the observations with the lower magnification sections (Fig. **3B**), *Nrf2*^{-/-} mice ameloblasts showed similar morphological appearance to the wild-type ameloblasts during the transition stage (Fig. **4A** and **C**). However, the *Nrf2*^{-/-} ameloblasts suffered from premature degenerative changes at the late maturation stage (Fig. **4D**; compare with those in the wild type mouse, Fig. **4B**) and the flat squamous epithelia largely disappeared in the mutant mouse tissues (data not

shown). These results thus demonstrate that the normal differentiation of ameloblasts are severely disturbed at the late maturation stage in the *Nrf2*^{-/-} mice.

Iron transport is defective in *Nrf2*^{-/-} mice

To examine whether the incomplete differentiation affects the ameloblasts function, iron metabolism during the ameloblast development was examined in *Nrf2*^{-/-} mice.

We carried out Berlin blue staining of wild type and *Nrf2*^{-/-} mouse incisors (Fig. 4, panels **E-H**). In the wild-type mouse incisors, positive staining of Berlin blue, which indicates the accumulation of iron, was detected in the ameloblast cytosol during the transition stage and early maturation stage (Fig. 4**E**). The accumulation of iron was then shifted to the plasma membrane on the enamel side at the late maturation stage, reflecting the iron excretion process into the enamel surface at this stage (Fig. 4**F**). No Berlin blue-positive staining was detected at the reduced ameloblast stage (data not shown). In the *Nrf2*^{-/-} enamel organ, iron was detected both in the papillary layer cells and ameloblasts during the transition and early maturation stages, and the iron accumulation in the ameloblast cytosol was markedly decreased (Fig. 4**G**). This may be due to defect of the iron transport from blood vessels to the ameloblasts.

We also found that the aberrant iron deposition overlapping with the degenerated cells (Fig. 4**H**), suggesting that the abnormal accumulation of iron might provoke, at least in part, the degeneration of papillary cells and ameloblasts of *Nrf2*^{-/-} enamel organ.

Ferritin expression was decreased in *Nrf2*^{-/-} papillary layer cells

Since ferritin is known to play an important role in the cellular iron metabolism, we next examined the expression the ferritin by immunohistochemical and *in situ* hybridization analyses. Ferritin heavy chain mRNA was expressed exclusively in the ameloblasts during transition and early maturation stages. The *Nrf2*^{-/-} ameloblasts show similar level expression to the wild-type ameloblasts (Fig. 5C and A, respectively). However, ferritin heavy chain mRNA expression was very faint or not observed in the late maturation stage and reduced ameloblast stage (data not shown) of the ameloblast development in both wild type and *Nrf2*^{-/-} mice (panels B and D, respectively).

We also performed immunohistochemical analysis of ferritin expression, utilizing an anti-rat liver ferritin antibody that cross-reacts with mouse ferritin (Miyazaki *et al.* 1998). The analysis revealed that the expression level of ferritin protein was comparable between ameloblasts and papillary layer cells at the transition and early maturation stages in the wild-type mouse (Fig. 5E). Importantly, however, in the *Nrf2*^{-/-} mouse the expression of ferritin in the papillary layer cells was significantly reduced compared to that in the ameloblasts (Fig. 5G). Consistent with the results of *in situ* ferritin heavy chain mRNA analysis, ferritin was expressed only faintly in the more advanced stages of ameloblasts (Fig. 5F and H). These results clearly indicate that although ferritin is expressed in the ameloblasts, it is not transferred efficiently from the ameloblasts to the papillary layer cells in *Nrf2*^{-/-} animals.

***Nrf2*^{-/-} teeth have decreased acid resistance**

To assess changes in the quality of the teeth, we first examined the Knoop hardness of the teeth. However, we could not detect significant difference between wild-type and *Nrf2*^{-/-} teeth. We next examined acid resistance of *Nrf2*^{-/-} teeth. For this purpose, the teeth were exposed to 0.1 M acetate buffer at pH 4.0 and amounts of eluted calcium ion were quantified at several time points by the methylxlenol blue method. As shown in Figure 6, the concentration of eluted calcium ion from *Nrf2*^{-/-} teeth was significantly higher than that from the wild-type teeth. The initial elution velocity increased rapidly, but the elution seems to be saturated at 30 and 40 min time points in *Nrf2*^{-/-} teeth. The calcium concentration level from the *Nrf2*^{-/-} teeth is significantly higher than that from the wild-type teeth (P<0.05: Student's t-test). Thus, the acid resistance of *Nrf2*^{-/-} teeth was significantly decreased compared to that of the wild-type mice, suggesting that the *Nrf2*^{-/-} teeth is susceptible to dental caries.

Discussion

Closer examination of the *Nrf2*^{-/-} mice unveiled that the surface color of maxillary incisors of the *Nrf2*^{-/-} mice is grayish white, which is a marked contrast to the yellowish brown color of the wild-type mouse incisors. Our analyses further revealed that this decolorization is due to the decrease in the iron content of the mature enamel. The analysis of iron metabolism in the enamel organ showed that the iron transport from blood vessels to the ameloblasts was disturbed in the *Nrf2*^{-/-} mouse during the ameloblast maturation stages. In the *Nrf2*^{-/-} mouse, ameloblasts underwent severe degenerative changes and disappeared prematurely during their maturation stages, so the loss of the ameloblast function resulted in the failure of iron deposition to the enamel surface and the decolorization of the incisors. To our knowledge, this is the first report describing the iron metabolism disorder in the *Nrf2*^{-/-} mouse.

Iron is critically involved in various cellular events ranging from DNA synthesis to cellular respiration (Cammack *et al.* 1990). Among them, the iron utilization in the rodent enamel organ illustrates one of the most interesting examples of iron usage in mammals. Iron deposited onto the enamel surface seems to contribute to the formation of acid resistance and hardness of the rodent incisors, which is advantageous for grinding the hard seeds in the environment (Halse *et al.* 1974; Stein *et al.* 1959). In fact, the diminished acid resistance of iron-poor *Nrf2*^{-/-} teeth (Fig. 6) supports the notion that the iron deposition to the enamel surface is an important

event to preserve the rodent tooth function.

In terms of the iron and calcium transport, as well as matrix and water removal, the papillary layer cells have been shown to form an intimate functional unit with the ameloblasts during early to late stages of the enamel maturation (Ohshima *et al.* 1998; Grant *et al.* 1968; Skobe *et al.* 1974). Importantly, transferrin receptors are found to be mainly expressed in the papillary layer cells of the enamel organ of rat incisors (Mataki *et al.* 1989), suggesting that the papillary layer cells uptake iron efficiently from the circulating blood. Although mechanism of the next transfer process of iron, *i.e.* from the papillary layer cells to ameloblasts, is not well understood at present, one plausible explanation for this is that the transferrin-bound iron from the circulating blood may be transferred to ferritin within the papillary layer cells, and subsequently the ferritin-bound iron is transferred to ameloblasts. Consistent with this contention, we observed high ferritin protein accumulation both in the ameloblasts and papillary layer cells in the wild-type enamel organ.

Ferritin serves as the transient iron reservoir in mature ameloblasts, and surprisingly the ameloblasts express ferritin mRNA most abundantly amongst rat tissues (Miyazaki *et al.* 1998). Ferritin is a 480-kDa intracellular protein that can store up to 4500 atoms of iron. The protein consists of heavy and light chains. The ratio of subunits within a ferritin molecule varies widely from tissue to tissue, which in turn modulates the ferritin function (Miyazaki *et al.* 1998). Although ferritin is expressed at equal levels both in

ameloblasts and papillary layer cells in the wild type enamel organ, the *in situ* analysis of ferritin heavy chain mRNA expression demonstrates that the mRNA is exclusively expressed in the ameloblasts. This observation suggests that the ferritin synthesized in the ameloblasts may be transferred to the papillary cells (Mataki, S. *et al.* 1989). An alternative, and less likely, possibility is that the expression of ferritin mRNA in papillary cells might be under the detection limit of the *in situ* hybridization method and efficient translation compensated for the weak expression of the gene at mRNA level.

While ferritin is abundantly accumulated, iron accumulation is scarcely observed in the papillary layer cells of the wild type mouse. This observation suggests that the iron transfer process from the papillary layer cells to ameloblasts may be very efficient in the wild-type enamel organ. We envisage that ferritin may be loaded with iron in the papillary layer cells and rapidly transferred to the ameloblasts.

An important observation is that the accumulation level of ferritin is abnormally reduced, but accumulation level of iron is abnormally increased, in the *Nrf2*^{-/-} papillary layer cells, suggesting that the iron transfer process is somehow disturbed in the *Nrf2*^{-/-} enamel organ. We envisage the following scenario to explain the observation, which is depicted schematically in Figure 7. Since the expression levels of ferritin heavy chain mRNA and ferritin protein in the *Nrf2*^{-/-} ameloblasts was almost comparable to those of the wild-type ameloblasts (see Fig. 5), a translocation or recycling step of ferritin from the ameloblasts to the papillary layer cells might

be affected in the *Nrf2*^{-/-} mice (Radisky *et al.* 1998; Kwok *et al.* 2003). Although the translocation of ferritin from ameloblasts to papillary layer cells has not been evidenced to date, such a mechanism might be affected in *Nrf2*^{-/-} enamel organ most probably because of the enhanced oxidative stress in ameloblasts.

An alternative explanation is that the decrease in the ferritin mRNA expression may be involved in the decrease of ferritin in the *Nrf2*^{-/-} papillary cells. Indeed, it was recently reported that the chemical activators of Nrf2 upregulates the ferritin heavy and light chain gene expression *in vivo*, indicating that the ferritin gene expression is under the regulation of Nrf2/ARE pathway (Primiano *et al.* 1996; Tsuji *et al.* 2000, Pietsch *et al.* 2003). Supporting this contention, it was also reported that the expression of ferritin genes is not induced, but basal level of the gene expression is rather reduced in *Nrf2*^{-/-} mouse embryonic fibroblasts (Pietsch *et al.* 2003). Moreover, decrease in the basal expression as well as the induction of ferritin gene was found in *Nrf2*^{-/-} astrocytes (Lee *et al.* 2003). The basal level expression of ferritin mRNA in *Nrf2*^{-/-} small intestine was also decreased in a microarray analysis (Thimmulappa *et al.* 2002). Thus, further analyses is required to clarify the underlying mechanisms of iron transport defect observed in *Nrf2*^{-/-} enamel organ.

The aberrant accumulation of iron in *Nrf2*^{-/-} papillary cells seems to lead the ameloblasts to premature degeneration by oxidative stress, as iron generates highly reactive oxygen species via Fenton chemistry and causes an oxidative stress to cells (Linn *et al.* 1998). Upon utilization of iron, therefore, cells need to be equipped with an array of antioxidant systems to prevent

its toxicity. Since Nrf2 regulates expression of the genes that protect cells from oxidative stress (Ishii *et al.* 2000; Itoh *et al.* 1999b), there is a possibility that defective expression of certain Nrf2/ARE-regulated gene(s) might be involved in the degenerative changes observed in the *Nrf2*^{-/-} enamel organ. For the understanding of the iron transport system that is defective in the *Nrf2*^{-/-} mouse, comprehensive as well as quantitative analyses of the expression of ARE-regulated genes in the enamel organ is critically important. However, we need a technical breakthrough for collecting enough amounts of mouse enamel organs for such analyses.

Experimental procedures

Macroscopic observation

The generation of *Nrf2* gene mutant mice was previously described (Itoh *et al.* 1997). The incidence of decolorization phenotype was analyzed by the chi square test.

Scanning electron microscopic observation and micro x-ray analysis

The murine incisors, including maxillary bones, were fixed in 100% ethanol and dehydrated by the critical point drying method. The incisors from *Nrf2*^{+/-} and *Nrf2*^{-/-} mice were examined using a scanning electron microscope (Hitachi S-2500CX) operated at 15 kV. Micro x-ray analysis was performed to determine the chemical components of the incisors. For energy-dispersive x-ray analysis, an x-ray detector system (Kevex Quantum Delta IV) attached to a scanning electron microscope was used. The micro x-ray analysis system was operated at a 15-kV accelerating voltage and a 0.1-nA probe current, with a 20- nm probe size and a 100-sec counting time. Five points on the enamel surface were selected and analyzed for the amounts of calcium, phosphorus and iron. The iron concentration was detected in 1 μm depth of enamel surface.

***In situ* hybridization, immunohistochemistry and iron staining**

Ferritin heavy chain cDNA was subcloned into the pBluescript KS⁺ vector and used as a template for cRNA production. DIG-11-UTP-labeled single-strand antisense and sense RNA probes were prepared by DIG-RNA Labeling Kit (Boehringer Mannheim) according to the manufacturer's instruction. Samples were fixed with

4% paraformaldehyde with PBS overnight at 4°C and decalcified in 10% EDTA (pH 7.4) for two weeks, embedded in paraffin and sectioned. *In situ* hybridization was performed as previously described (Shibata *et al.* 2000). After treatment with 0.2 N hydrochloric acid and Proteinase K (10 µg /ml), hybridization was performed with the probe (1 µg/ml) at 50° C overnight. After extensive washing and RNase A treatment, the hybridized DIG-labeled probes were detected with alkaline phosphatase-conjugated anti-DIG antibody and 5-bromo-4-chloro-3-indolyl phosphate as the substrate, using a nucleic acid detection kit (Boehringer Mannheim).

Immunostaining was performed using the labeled streptavidin biotin method (LsAB method: Nichirei). Sections were immersed in 0.3% hydrogen peroxide in methanol for 30 min, and incubated with 5% normal goat serum for 30 min at room temperature. The sections were then incubated with anti-rat liver ferritin rabbit polyclonal antibody (1:200 v/v) in PBS at 4°C overnight (Miyazaki *et al.* 1998). The slides were reacted with biotinylated goat anti-rabbit antibody for 30 min at room temperature, followed by horseradish peroxidase conjugated with streptavidin. The peroxidase activity was visualized by the 3-amino-9-ethylcarbasol substrate-chromogen system (Nichirei, Tokyo). The sections were counterstained with hematoxylin, dehydrated, and mounted. Control staining was performed with non-immune rabbit serum. Berlin blue staining was performed to detect iron deposits.

Serum iron parameters and liver iron content

Blood was obtained from abdominal aorta of anesthetized mice and 200 μ l of serum from each animal was used for analysis of iron and total iron binding capacity. These assays were performed by SRL Inc. (Tokyo) using an automatic chemical analyzer (Hitachi). Non-heme iron in the liver was measured as previously described (Foy et al. 1967).

Analysis of acid resistance and Knoop hardness

Hardness test of the enamel surface was performed by using a hardness tester equipped with a Knoop diamond penetrator. Six kg load was applied to each tooth for 10 s. To measure the acid resistance of the teeth, a 5 mm x 0.5 mm of the buccal surface of the murine incisors was exposed to 100 μ l of acetate buffer (100 mM) at pH 4.0 at room temperature. The eluted calcium ion was measured by the methylxyleneol blue method (Calcium E test Wako, Wako) at 5, 10, 15, 20, 30 and 40 min. The means from five independent incisors from 8-12 week old mice were presented with standard errors.

Acknowledgements

We thank Dr. Takanobu Isokawa and Kit I. Tong for discussion and advice. This work was supported in part by grants from JST-ERATO, JSPS, the Ministry of Education, Science, Sports and Technology, the Ministry of Health, Labor and Welfare, CREST, and the Naito foundation.

References

- Aoki, Y., Sato, H., Nishimura, N., Takahashi, S., Itoh, K. & Yamamoto, M. (2001) Accelerated DNA adduct formation in the lung of the Nrf2 knockout mouse exposed to diesel exhaust. *Toxicol. Appl. Pharmacol.* **173**, 154-160.
- Cammack, R., Wriggleworth, J. M. & Baum, H. (1990) Iron dependent enzymes in mammalian systems. In: Iron Transport and Storage (eds. P. Ponka, H. M. Schulman & R. C. Woodworth), pp. 17-40. Boca Raton: CRC Press.
- Chan, K. & Kan, Y. W. (1999) Nrf2 is essential for protection against acute pulmonary injury in mice. *Proc. Natl. Acad. Sci. U S A* **96**, 12731-12736.
- Chan, K., Han, X. D. & Kan, Y. W. (2001) An important function of Nrf2 in combating oxidative stress: detoxification of acetaminophen. *Proc. Natl. Acad. Sci. U S A*. **98**, 4611-4616.
- Cho, H. Y., Jedlicka, A. E., Reddy, S. P., et al. (2002) Role of NRF2 in Protection Against Hyperoxic Lung Injury in Mice. *Am. J. Respir. Cell. Mol. Biol.* **26**, 175-182.
- Enomoto, A., Itoh, K., Nagayoshi, E., et al. (2001) High sensitivity of Nrf2 knockout mice to acetaminophen hepatotoxicity associated with decreased expression of ARE-regulated drug metabolizing enzymes and antioxidant genes. *Toxicol. Sci.* **59**, 169-177.
- Foy, A. L., Williams, H. L., Cortell, S. & Conrad, M. E. (1967) A modified procedure for the determination of nonheme iron in tissue. *Analytical Biochemistry.* **18**, 559-563.
- Garant, P. R. & Gillespie, R. (1969) The presence of fenestrated

- capillaries in the papillary layer of the enamel organ. *Anat. Rec.* **163**, 71-79.
- Halse, A. (1973) Effect of dietary iron deficiency on the pigmentation and iron content of rat incisor enamel. *Scand. J. Dent. Res.* **81**, 319-334.
- Halse, A. (1974) Electron microprobe analysis of iron content of incisor enamel in some species of Rodentia. *Arch. Oral. Biol.* **19**, 7-11.
- Halse, A. & Selvig, K. A. (1974) Incorporation of iron in rat incisor enamel. *Scand. J. Dent. Res.* **82**, 47-56.
- Ishii, T., Itoh, K., Takahashi, S., et al. (2000) Transcription factor Nrf2 coordinately regulates a group of oxidative stress-inducible genes in macrophages. *J. Biol. Chem.* **275**, 16023-16029.
- Itoh, K., Igarashi, K., Hayashi, N., Nishizawa, M. & Yamamoto, M. (1995) Cloning and characterization of a novel erythroid cell-derived CNC family transcription factor heterodimerizing with the small maf family proteins. *Mol. Cell. Biol.* **15**, 4184-4193.
- Itoh, K., Chiba, T., Takahashi, S., et al. (1997) An Nrf2/small maf heterodimer mediates the induction of phase II detoxifying enzyme genes through antioxidant responsive element. *Biochem. Biophys. Res. Commun.* **236**, 313-322.
- Itoh, K., Ishii, T., Wakabayashi, N. & Yamamoto, M. (1999a) Regulatory mechanisms of cellular response to oxidative stress. *Free Radic. Res.* **31**, 319-324.
- Itoh, K., Wakabayashi, N., Katoh, Y., et al. (1999b) Keap1 represses nuclear activation of antioxidant responsive elements by Nrf2 through binding to the amino-terminal Neh2 domain. *Genes Dev.* **13**, 76-86.
- Kallenbach, E. (1970) Fine structure of rat incisor enamel organ during late pigmentation

- and regression stages. *J. Ultrastruct. Res.* **30**, 38-63.
- Karim, A. & Warshawsky, H. (1984) A radioautographic study of the incorporation of iron 55 by the ameloblasts in the zone of maturation of rat incisors. *Am. J. Anat.* **169**, 327-335.
- Kuroha, T., Takahashi, S., Komeno, T., Itoh, K., Nagasawa, T. & Yamamoto, M. (1998) Ablation of Nrf2 function does not increase the erythroid or megakaryocytic cell lineage dysfunction caused by p45 NF-E2 gene disruption. *J. Biochem.* **123**, 376-379.
- Kwok, J. C. & Richardson, D. R. (2003) Anthracyclines induce accumulation of iron in ferritin in myocardial and neoplastic cells: inhibition of the ferritin iron mobilization pathway. *Mol. Pharmacol.* **63**, 849-861.
- Lee, J. M., Calkins, M. J., Chan, K., Kan, Y. W. & Johnson, J. A. (2003) Identification of the NF-E2-related factor-2-dependent genes conferring protection against oxidative stress in primary cortical astrocytes using oligonucleotide microarray analysis. *J. Biol. Chem.* **278**, 12029-12038.
- Linn, S. (1998) DNA damage by iron and hydrogen peroxide in vitro and in vivo. *Drug Metab. Rev.* **30**, 313-326.
- Mataki, S., Ohya, M., Kubota, M., Ino, M. & Ogura, H. (1989) Immunohistochemical and pharmacological studies on the distribution of ferritin and its secretory process of ameloblasts in rat incisor enamel. In: *Tooth enamel* (ed. R. W. Fearnhead), pp. 108-112. Yokohama: Yokohama Florence Publishers.
- Miyazaki, Y., Sakai, H., Shibata, Y., Shibata, M., Mataki, S. & Kato, Y.

- (1998) Expression and localization of ferritin mRNA in ameloblasts of rat incisor. *Arch. Oral. Biol.* **43**, 367-378.
- McCord, J. M. (1998) Iron, free radicals, and oxidative injury. *Semin. Hematol.* **35**, 5-12.
- Mohler, J., Vani, K., Leung, S. & Epstein, A. (1991) Segmentally restricted, cephalic expression of a leucine zipper gene during *Drosophila* embryogenesis. *Mech. Dev.* **34**, 3-9.
- Ohshima, H., Maeda, T. & Takano, Y. (1998) Cytochrome oxidase activity in the enamel organ during amelogenesis in rat incisors. *Anat. Rec.* **252**, 519-531.
- Pietsch, E. C., Chan, J. Y., Torti, F. M. & Torti, S. V. (2003) Nrf2 mediates the induction of ferritin H in response to xenobiotics and cancer chemopreventive dithiolethiones. *J. Biol. Chem.* **278**, 2361-2369.
- Primiano, T., Kensler, T. W., Kuppusamy, P., Zweier, J. L. & Sutter, T. R. (1996) Induction of hepatic heme oxygenase-1 and ferritin in rats by cancer chemopreventive dithiolethiones. *Carcinogenesis.* **17**, 2291-2296.
- Radisky, D. C. & Kaplan, J. (1998) Iron in cytosolic ferritin can be recycled through lysosomal degradation in human fibroblasts. *Biochem. J.* **336**, 201-215.
- Ramos-Gomez, M., Kwak, M. K., Dolan, P. M., et al. (2001) Sensitivity to carcinogenesis is increased and chemoprotective efficacy of enzyme inducers is lost in nrf2 transcription factor-deficient mice. *Proc. Natl. Acad. Sci. USA* **98**, 3410-3415.
- Shibata, Y., Fujita, S., Takahashi, H., Yamaguchi, A. & Koji, T. (2000) Assessment of decalcifying protocols for detection of specific RNA by non-radioactive in

situ hybridization in calcified tissues. *Histochem. Cell Biol.* **113**, 153-159.

Skobe, Z. & Garant, P. R. (1974) Electron microscopy of horseradish peroxidase uptake by papillary cells of the mouse incisor enamel organ. *Arch. Oral Biol.* **19**, 387-395.

Stein, G. & Boyle, P. E. (1959) Pigmentation of the enamel of albino rat incisor teeth. *Arch. Oral Biol.* **1**, 97-105.

Takano, Y. & Ozawa H. (1981) Cytochemical studies on the ferritin-containing vesicles of the rat incisor ameloblasts with special reference to the acid phosphatase activity. *Calcif. Tissue Int.* **33**, 51-55.

Thimmulappa, R. K., Mai, K. H., Srisuma, S., Kensler, T. W., Yamamoto, M. & Biswal, S. (2002) Identification of Nrf2-regulated genes induced by the chemopreventive agent sulforaphane by oligonucleotide microarray. *Cancer Res.* **62**, 5196-5203.

Tsuji, Y., Ayaki, H., Whitman, S. P., Morrow, C. S., Torti, S. V. & Torti, F. M. (2000) Coordinate transcriptional and translational regulation of ferritin in response to oxidative stress. *Mol. Cell Biol.* **20**, 5818-5827.

Yoh, K., Itoh, K., Enomoto, A., et al. (2001) Nrf2 deficient female mice develop lupus-like autoimmune nephritis. *Kidney Int.* **60**, 1343-1353.

Table 1. Micro x-ray analysis of the incisors of *Nrf2*^{-/-} mutant mice

	Nrf2 genotype		
	+/+	+/-	-/-
Fe (% (w/w))	5.143±0.754	2.748±0.454*	0.396±0.076 *
Ca (% (w/w))	36.389±0.222	36.073±0.039	36.161±0.067
P (% (w/w))	18.057±0.091	17.808±0.104	17.954±0.047
Ca/P WR	2.0158±0.006	2.0262±0.011	2.0149±0.007
Ca/P MR	1.5578±0.005	1.5659±0.008	1.5550±0.007

The calcium, phosphorus, and iron contents of the enamel surface of wild-type, *Nrf2*^{+/-}, or *Nrf2*^{-/-} incisors determined by micro x-ray analysis. The means from five incisors are presented with standard deviations. Student's t-test was used for the statistical analysis. Asterisks indicate significant difference compared with wild type ($P < 0.001$).

Table 2. General iron status of *Nrf2*^{-/-} mice

	Nrf2 genotype	
	+/+	-/-
Hematocrit (%)	52.2±2.9	52.7±2.9
Serum iron (μg/dl)	219.5±40.6	271.0±50.5
TIBC (μg/dl)	407.8±52.6	460.3±71.2
Transferrin saturation (%)	54.4±11.8	59.1±8.7
Liver iron content (ng/mg)	55.0±18.0	90.0±11.7*

Hematocrit, serum iron concentration, total iron binding capacity (TIBC), transferrin saturation and liver iron content were measured in wild-type and *Nrf2*^{-/-} mice. The means from 6 mice are presented with standard deviations. Student's t-test was used for the statistical analysis. Asterisks indicate significant difference compared with wild type ($P < 0.01$).

Figure legends

Figure 1 Incisors of *Nrf2*^{-/-} mice are decolorized. The incisors of wild-type mouse show the normal brownish-yellow color (A), whereas the incisors of *Nrf2*^{-/-} mice have grayish white color (B).

Figure 2 Scanning electron microscopic and micro x-ray analysis of the surface of the mouse incisor. (A and D) Scanning electron microscopic images of incisors of wild-type (A) and *Nrf2*^{-/-} mouse (D). (B and E) Dot-map images of calcium on the surface of wild-type (B) and *Nrf2*^{-/-} incisors (E) by micro x-ray analysis. (C and F) Dot-map images of iron on the surface of wild-type (C) and *Nrf2*^{-/-} mouse incisors (F).

Figure 3 *Nrf2*^{-/-} ameloblasts show degenerative atrophy at the late maturation stage. (A and B) Hematoxylin and eosin staining of wild type (A) and *Nrf2*^{-/-} (B) mouse enamel organs. The ameloblasts of *Nrf2*^{-/-} mouse show severe premature degenerative atrophy at the late maturation stage (40 x original magnification). Abbreviations are **t**, transition stage; **em**, early maturation stage; **lm**, late maturation stage; **ra**, region of reduced ameloblasts.

Figure 4 Defective iron transport in *Nrf2*^{-/-} mouse enamel organ. (A to D) Hematoxylin and eosin staining of wild type (A and B) and *Nrf2*^{-/-} (C and D) mouse enamel organs. (E to H) Berlin blue staining of wild type (E and F) and *Nrf2*^{-/-} (G and H) mouse enamel organs. Panels A, C, E and G show the transition stage,

while panels B, D, F and H show the late maturation stage of ameloblast maturation. **AM**, ameloblasts; **PA**, Papillary cell layer.

Figure 5 Expression of ferritin and ferritin heavy chain mRNA in *Nrf2*^{-/-} enamel organ. (A to D) In situ hybridization analysis of ferritin heavy chain mRNA of wild type (A and B) and *Nrf2*^{-/-} (C and D) mouse enamel organs. (E to H) Immunohistochemical analysis of ferritin in the wild type (E and F) and *Nrf2*^{-/-} (G and H) mouse enamel organs. Panels A, C, E and G show the transition stage, while panels B, D, F and H show the late maturation stage of ameloblast maturation. **AM**, ameloblasts; **PA**, Papillary cell layer.

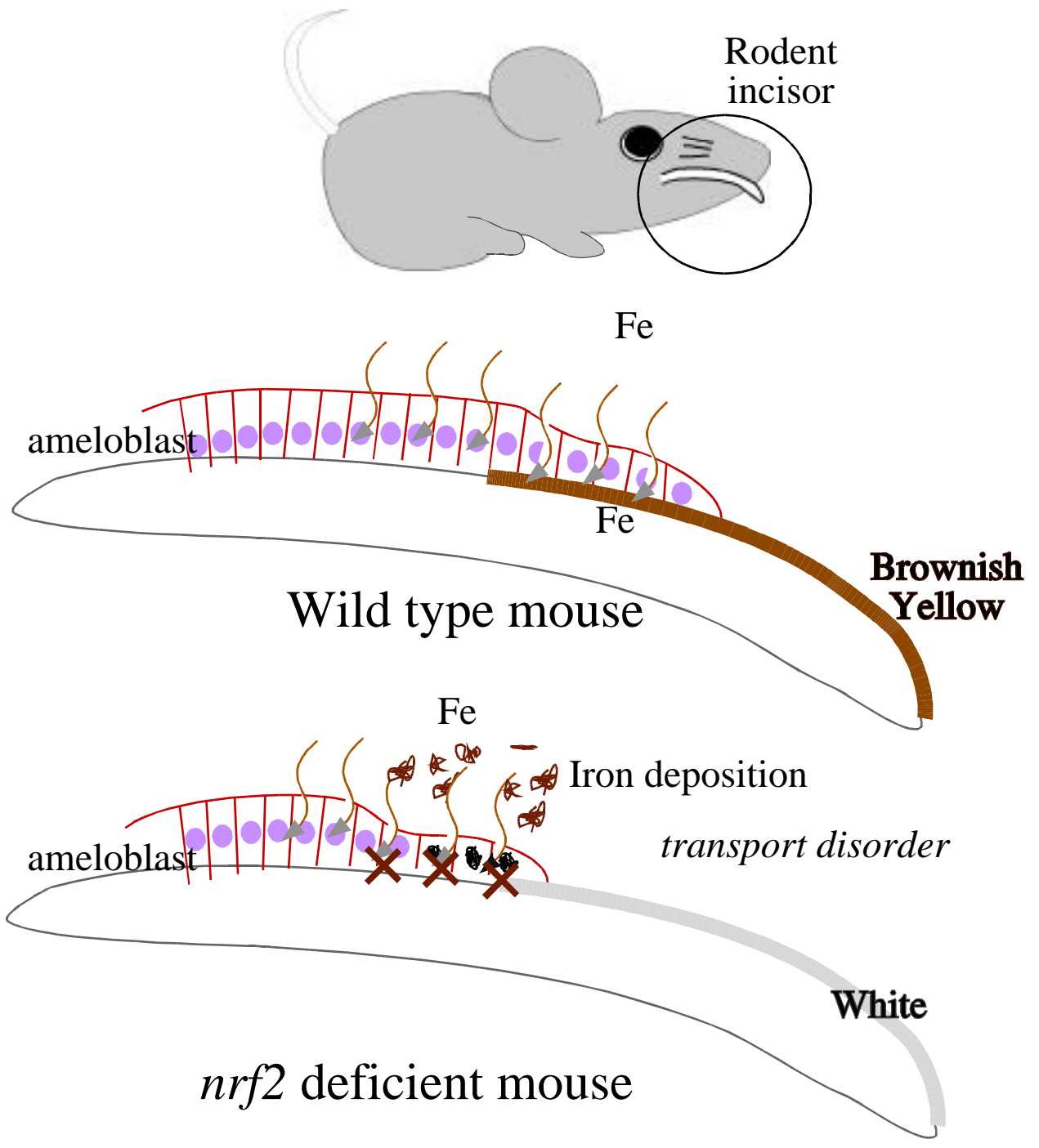
Figure 6 *Nrf2*^{-/-} mice incisors have diminished acid resistance.

A 0.5 mm x 5 mm area of the buccal surface of murine incisors was exposed to acetate buffer at pH 4.0, and the amount of eluted calcium ion was determined. The surface of the *Nrf2*^{-/-} tooth (open square) eroded significantly earlier in acetic acid than that of the wild-type mice (open circle). * P<0.05: Student's t-test.

Figure 7 *Nrf2*^{-/-} mice were defective in iron utilization in developing enamel organ.

Nrf2^{-/-} teeth were grayish white (bottom panel), whereas those of wild type mice were brownish yellow (middle panel). This decolorization is owing to the defect of iron deposition in the mature enamel surface. *Nrf2*^{-/-} enamel organs have iron transport defect that leads to both enamel cell degeneration and

disturbed iron deposition onto the enamel surface. Brown arrows designate the direction of iron transport and subsequent deposition.



Summary figure



Fig.1

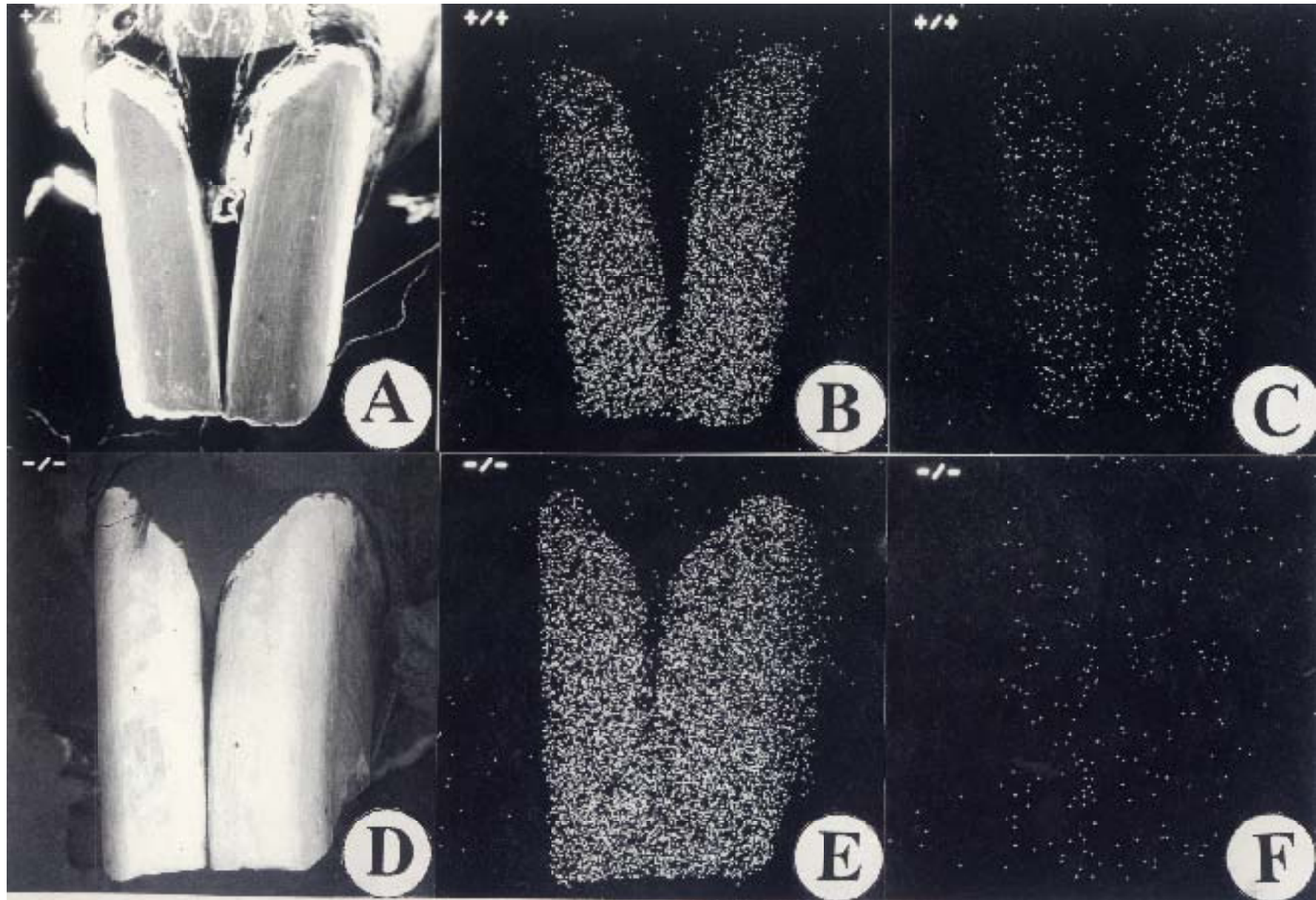


Fig.2

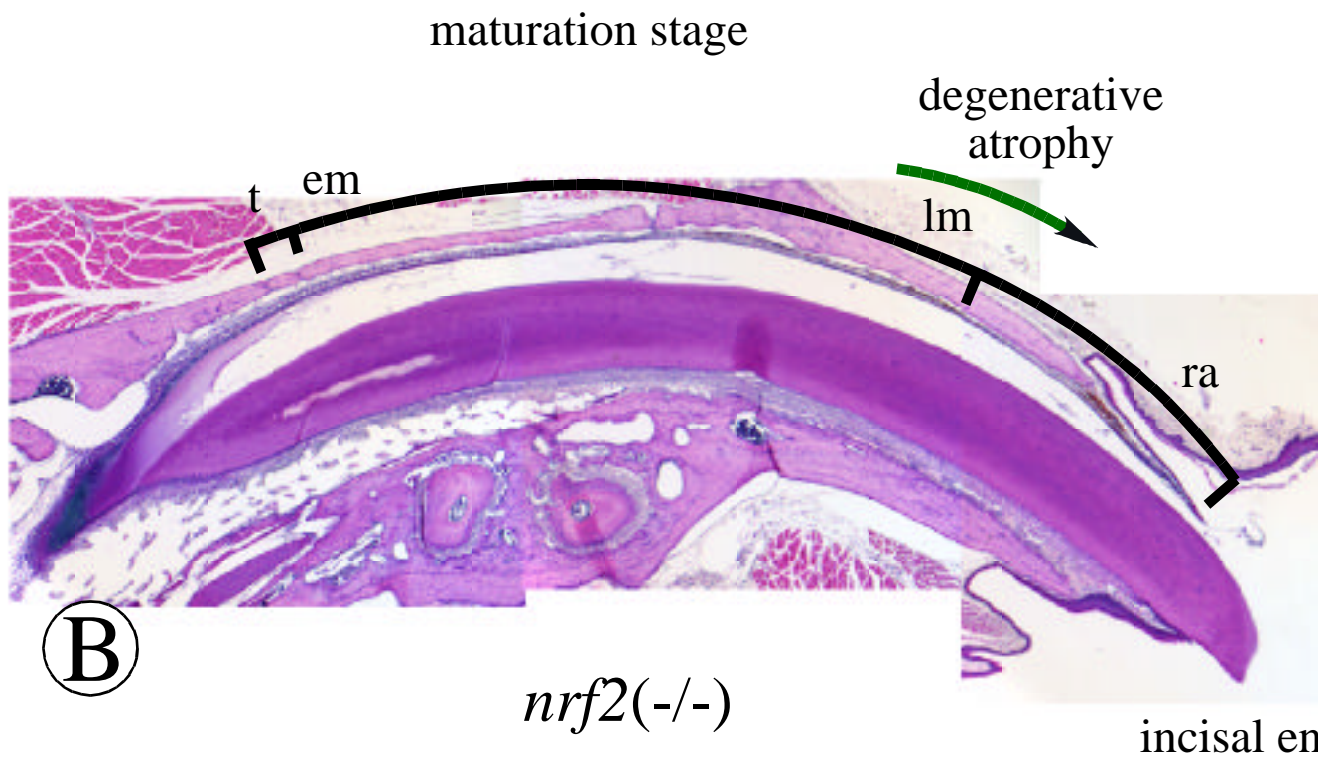
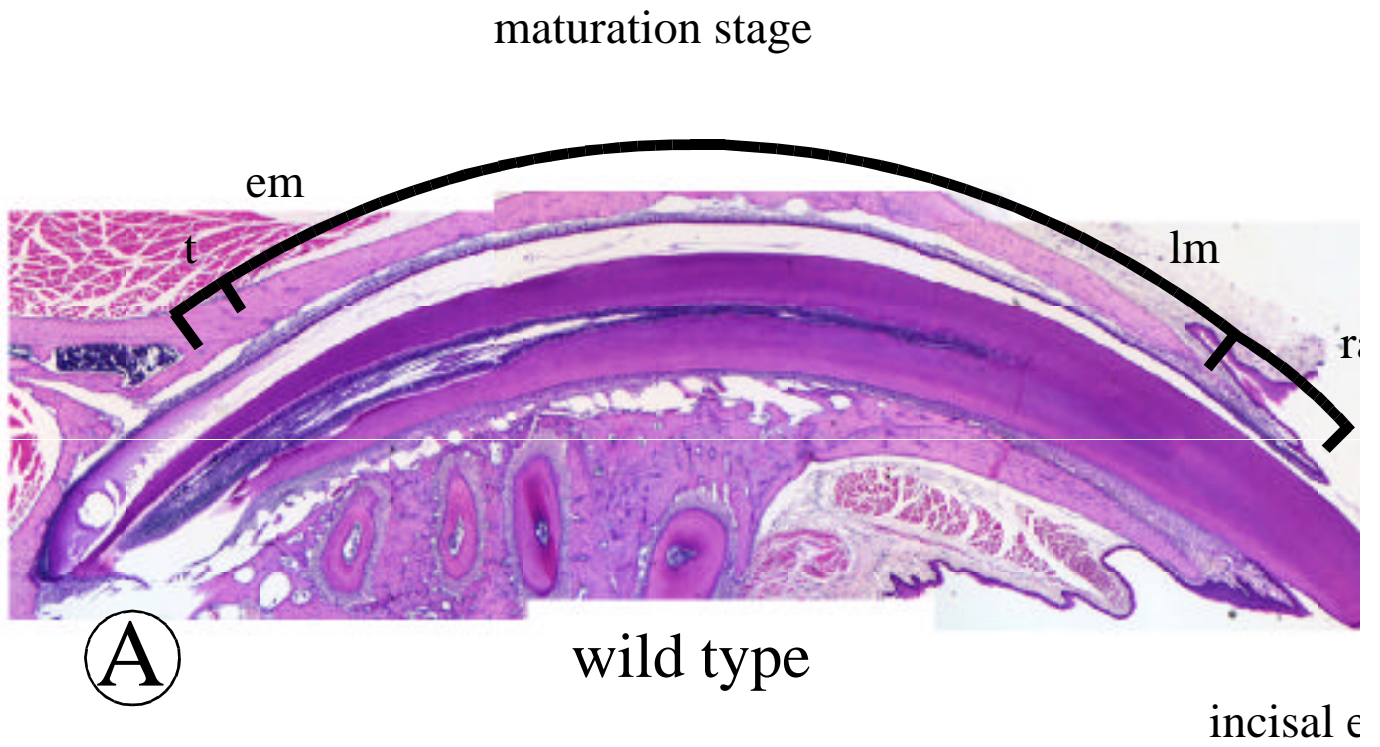
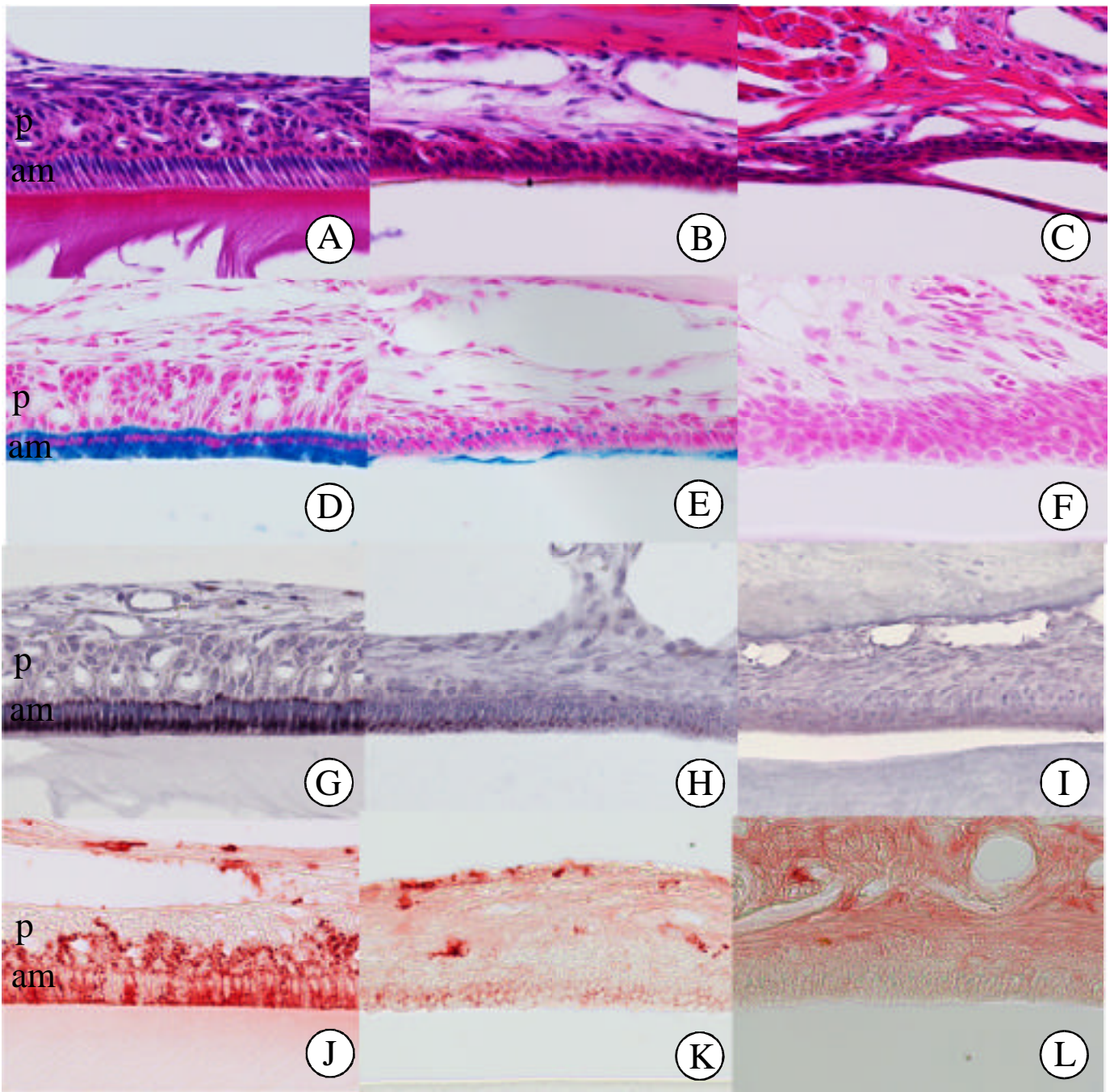


Figure 3

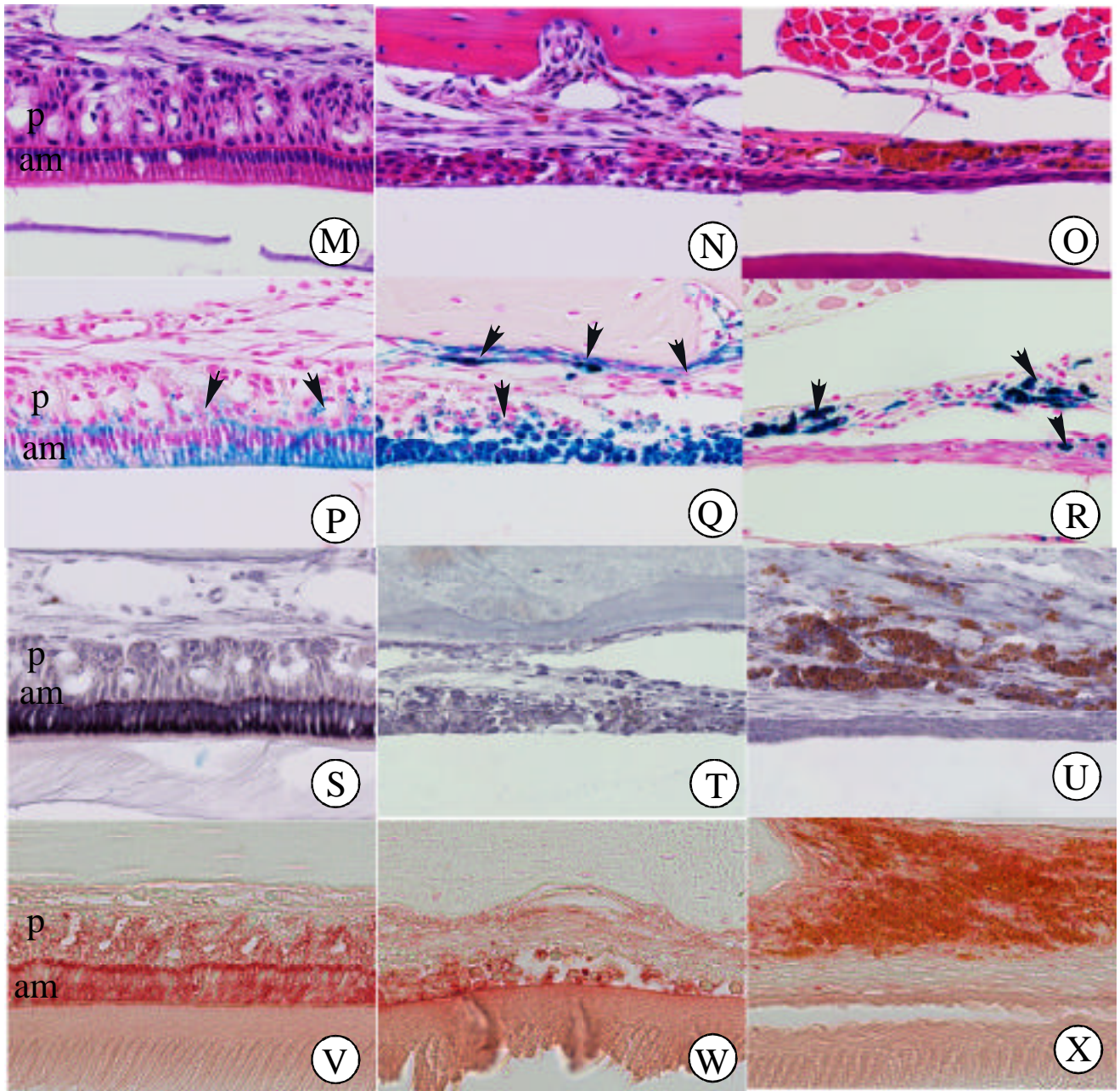


Transition~early
maturation stage

Late maturation
stage

Region of reduced
ameloblasts

Figure 4 (A-L)



Transition~early maturation stage

Late maturation stage

Region of reduced ameloblasts

Figure 4 (M-X)

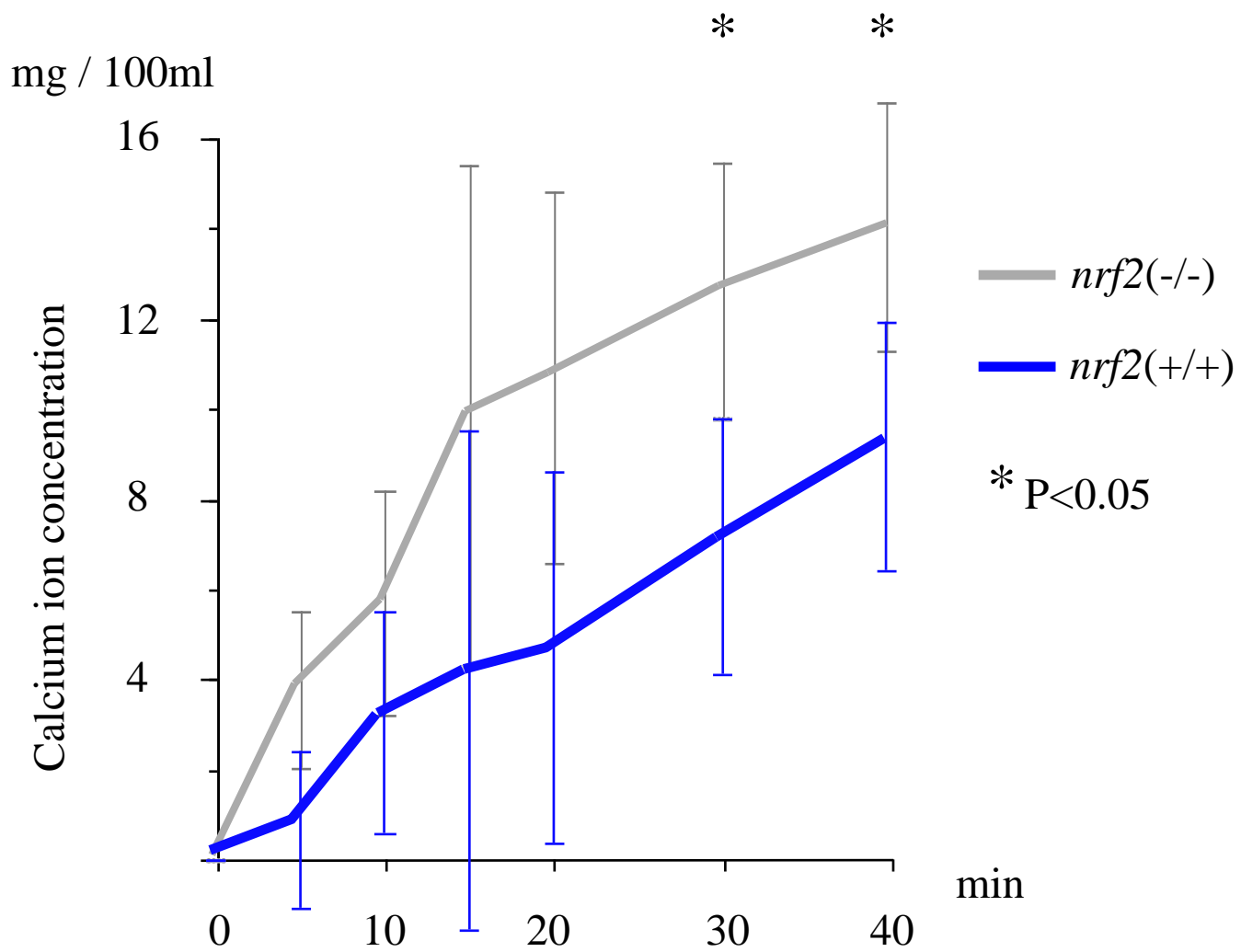


Figure 5